Optimum Design of a Gravitationally Oriented Two-Body Satellite

By E. Y. YU

Optimum ranges of the inertia ratios, the spring constants, and the damping constants have been obtained for the design of a gravitationally oriented two-body satellite with satisfactory over-all damping performance. In the case of viscous damping, optimum damping constants can be simply chosen from diagrams of complex root loci. It is found impossible to convert the optimum viscous damping constants into optimum magnetic hysteresis damping constants, and the latter have to be obtained from computer solutions. The result of this optimization work makes possible a better design of the satellite with lighter attitude control weight, shorter rod lengths, and smaller earth-pointing error than previously reported in articles in the Bell System Technical Journal.

I. INTRODUCTION

The dynamics analysis by Fletcher, Rongved, and Yu[1] has shown that a two-body satellite will achieve an earth-pointing motion from an initial tumbling as a result of energy dissipation in the hinge joint through the relative motion between the two bodies. For a practical application, we shall consider the earth-pointing body to be like a dumbbell and the auxiliary body like a sheet, the two being connected to each other through a hinge mechanism of universal-joint type to allow a two-degree-of-freedom relative motion. When the satellite is in an earth-pointing motion, the auxiliary body is parallel to the local horizontal in its unstable orientation, and the two axes of relative motions are aligned with the roll and pitch direction (see Fig. 1). The over-all aspect of such a passive gravitational attitude control system has been studied by Paul, West, and Yu[2] employing the magnetic hysteresis damping mechanism. Certain designs of the satellite in terms of moments of inertia, spring constants, and damping constants have been given in both Refs. 1 and 2 for an altitude of 6000 nautical miles (nm). They
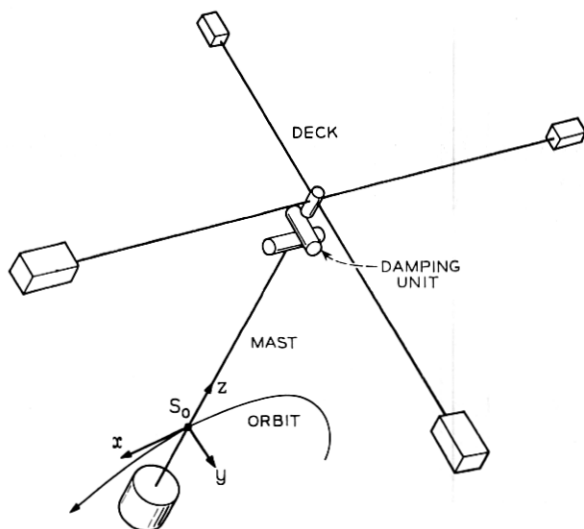
Fig. 1 — Two-body satellite configuration.

are found workable, but by no means "optimum," which means the achievement of the best over-all damping performance in tumbling motion, large-angle motion, torque-free librations, and forced librations under environmental torques of various frequencies.

The present work concerns a parameter optimization of the afore-mentioned two-body satellite employing two types of damping: the linear velocity of viscous type, and the nonlinear magnetic hysteresis type. With damping of the viscous type, analytical results can be obtained for the librational motions which may be used as a basis of parameter design in the case of magnetic hysteresis damping. The employment of magnetic hysteresis damping even makes the (linearized) equations of librational motions highly nonlinear, such that analytical treatment becomes intractable and results have to be obtained by numerical means.

II. GENERAL EQUATIONS OF MOTION

The equations of rotational motion which have been derived in Ref. 1 will be repeated here. The coordinate systems, as indicated in Fig. 2, are defined as follows. Let O-XYZ be a nonrotating frame, with its origin at the geocenter O, its Z-axis passing through the perigee of the orbit, and its Y-axis parallel to the orbital angular momentum vector.

Let S_o-xyz be an earth-pointing frame, with its origin S_o at the center of mass of the composite satellite, with z axis parallel to OS_o (the local vertical) making an angle ψ with OZ and with the y axis parallel to OY. The body coordinates of body 1, S_1-$x_1 y_1 z_1$, are defined along its principal axes, with adjusted[1] moments of inertia (I_1, I_2, I_3). Euler parameters (ξ, η, ζ, χ) are employed to describe the motion of S_1-$x_1 y_1 z_1$ relative to S_o-xyz. The matrix of transformation from the latter to the former frame is given as

$$[a_{ij}] = \begin{bmatrix} \xi^2 - \eta^2 - \zeta^2 + \chi^2 & 2(\xi\eta + \zeta\chi) & 2(\xi\zeta - \eta\chi) \\ 2(\xi\eta - \zeta\chi) & -\xi^2 + \eta^2 - \zeta^2 + \chi^2 & 2(\xi\chi + \eta\zeta) \\ 2(\xi\zeta + \eta\chi) & 2(-\xi\chi + \eta\zeta) & -\xi^2 - \eta^2 + \zeta^2 + \chi^2 \end{bmatrix}. \quad (1)$$

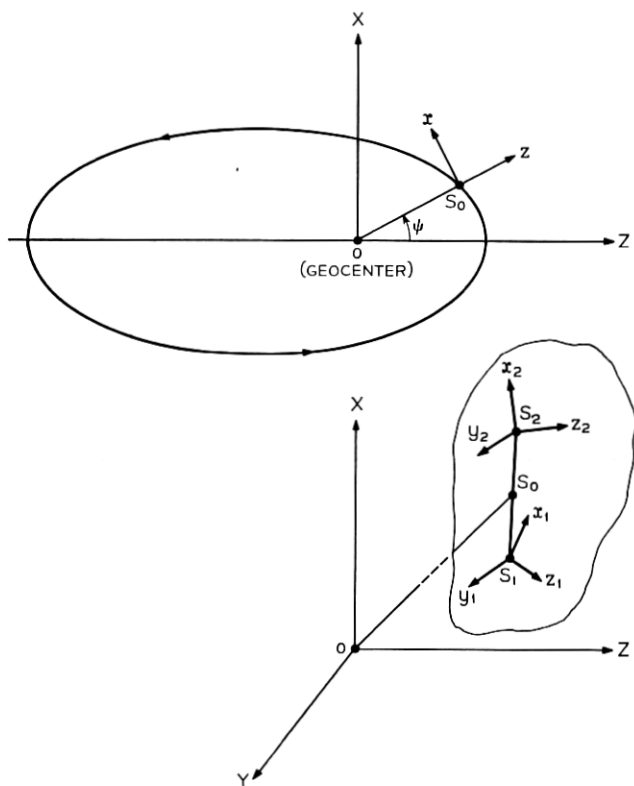Among the Euler parameters the relation $\xi^2 + \eta^2 + \zeta^2 + \chi^2 = 1$ holds.

Fig. 2 — Coordinate systems.

The coordinates S_2-$x_2y_2z_2$ are defined along the principal axes of body 2, with moments of inertia (I_4, I_5, I_6). The rotation of body 2 relative to body 1 is specified by an angle, α, about the x_1 axis and then an angle, β, about the y_2 axis. The transformation matrix from S_1-$x_1y_1z_1$ to S_2-$x_2y_2z_2$ is

$$[b_{ij}] = \begin{bmatrix} C\beta & S\alpha S\beta & -C\alpha S\beta \\ 0 & C\alpha & S\alpha \\ S\beta & -S\alpha C\beta & C\alpha C\beta \end{bmatrix}, \tag{2}$$

where C and S are abbreviations of cosine and sine, respectively.

The equations of motion of the two-body satellite with the hinge joint situated at the center of mass of the auxiliary body and at the earth-pointing z_1 axis of the satellite body are:

$$I_1\dot{\omega}_1 = (I_2 - I_3)(\omega_2\omega_3 - Gn_2n_3) + T_{r1} + T_{d1}, \tag{3a}$$

$$I_2\dot{\omega}_2 = (I_3 - I_1)(\omega_3\omega_1 - Gn_3n_1) + (T_{r2} + T_{d2})C\alpha \\ - T_cS\alpha, \tag{3b}$$

$$I_3\dot{\omega}_3 = (I_1 - I_2)(\omega_1\omega_2 - Gn_1n_2) + (T_{r2} + T_{d2})S\alpha \\ + T_cC\alpha, \tag{3c}$$

$$I_4\dot{\omega}_4 = (I_5 - I_6)(\omega_5\omega_6 - Gn_5n_6) - (T_{r1} + T_{d1})C\beta \\ + T_cS\beta, \tag{3d}$$

$$I_5\dot{\omega}_5 = (I_6 - I_4)(\omega_6\omega_4 - Gn_6n_4) - T_{r2} - T_{d2}, \tag{3e}$$

$$I_6\dot{\omega}_6 = (I_4 - I_5)(\omega_4\omega_5 - Gn_4n_5) - (T_{r1} + T_{d1})S\beta \\ - T_cC\beta. \tag{3f}$$

In the above, $(\omega_1, \omega_2, \omega_3)$ are the components of the total angular velocity of body 1 along S_1-$x_1y_1z_1$, and $(\omega_4, \omega_5, \omega_6)$ are those of body 2 along S_2-$x_2y_2z_2$. The coefficient G involves orbital elements: i.e.,

$$G = 3\Omega^2(1 - \epsilon^2)^{-3}(1 + \epsilon C\psi)^3,$$

where ϵ = orbital eccentricity, and $\Omega = 2\pi$ divided by the orbital period. Also,

$$n_i = a_{i3}, \quad n_{i+3} = \sum_{k=1}^{3} b_{ik}a_{k3}, \quad i = 1, 2, 3,$$

with a_{ij} and b_{ij} the elements of the transformation matrices (1) and (2). The constraint torque, T_c, is given as

$$
T_c = \left(\frac{S^2\alpha}{I_2} + \frac{C^2\alpha}{I_3} + \frac{S^2\beta}{I_4} + \frac{C^2\beta}{I_6} \right)^{-1}
$$

$$
\cdot \left\{ \frac{S\alpha}{I_2} \left[(I_3 - I_1)(\omega_1\omega_3 - Gn_1n_3) + (T_{r2} + T_{d2})C\alpha \right] \right.
$$

$$
- \frac{C\alpha}{I_3} \left[(I_1 - I_2)(\omega_1\omega_2 - Gn_1n_2) + (T_{r2} + T_{d2})S\alpha \right]
$$

$$
- \frac{S\beta}{I_4} \left[(I_5 - I_6)(\omega_5\omega_6 - Gn_5n_6) - (T_{r1} + T_{d1})C\beta \right] \tag{4}
$$

$$
+ \frac{C\beta}{I_6} \left[(I_4 - I_5)(\omega_4\omega_5 - Gn_4n_5) - (T_{r1} + T_{d1})S\beta \right]
$$

$$
\left. + \dot\alpha(\omega_2 C\alpha + \omega_3 S\alpha) - \dot\beta(\omega_4 C\beta + \omega_6 S\beta) \right\}.
$$

The restoring torques T_{r1} and T_{r2} acting on body 1 along the x_1 and y_2 axes, respectively, are linear with the relative angle of rotation: i.e., $T_{r1} = k_1\alpha$, $T_{r2} = k_2\beta$, where k_1 and k_2 are spring constants. The damping torques acting on body 1, T_{d1} and T_{d2}, along the x_1 and y_2 axes, respectively, are defined in the following. For viscous damping, $T_{d1} = C_1\dot\alpha$, and $T_{d2} = C_2\dot\beta$, where C_1 and C_2 are viscous damping coefficients. For magnetic hysteresis damping, the torque is dependent on the history of motion and is defined in regions I and III of Fig. 3 for T_{d2} as

$$
T_{d2} = T_{d2}^* + \bar{T}_{d2} \frac{\beta - \beta^*}{\bar\beta}, \tag{5}
$$

as long as $|T_{d2}| < \bar{T}_{d2}$, where $\bar\beta$, $\bar{T}_{d2}$ are constants, and β^*, T_{d2}^* are the values of β, T_{d2} when $\dot\beta$ last changed sign. After $|T_{d2}|$ reaches $\bar{T}_{d2}$ then T_{d2} remains at $\bar{T}_{d2}$ as long as $\dot\beta$ does not change sign, as represented in regions II and IV of Fig. 3. The magnitudes of $\bar\beta$ and $\bar{T}_{d2}$ will be given in Section IV, where the minor loops will be described. According to the major loop in Fig. 3, no energy dissipation will result if the amplitude of oscillation is less then $\bar\beta$. T_{d1} is defined by replacing β by α and subscript 2 by 1 in (5).

It can be shown that the Euler parameters and the relative angles of rotation are related to the ω_i's, $i = 1, \cdots, 6$, as follows:

$$
\dot\xi = \tfrac{1}{2}(\chi\lambda_1 - \zeta\lambda_2 + \eta\lambda_3), \tag{6a}
$$

$$
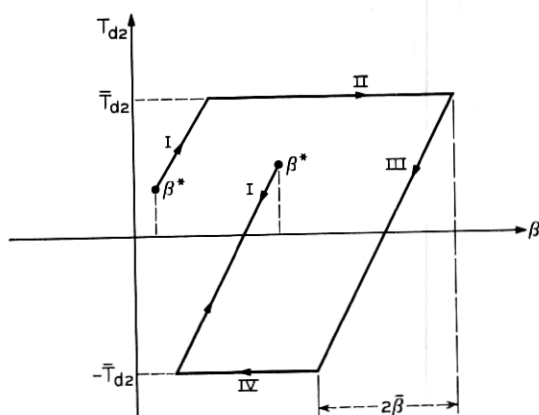\dot\eta = \tfrac{1}{2}(\zeta\lambda_1 + \chi\lambda_2 - \xi\lambda_3), \tag{6b}
$$

Fig. 3 — Magnetic hysteresis damping torque vs amplitude, $T_{d2} - \beta$.

$$\dot{\zeta} = \tfrac{1}{2}(-\eta\lambda_1 + \xi\lambda_2 + \chi\lambda_3), \tag{6c}$$

$$\dot{\chi} = \tfrac{1}{2}(-\xi\lambda_1 - \eta\lambda_2 - \zeta\lambda_3), \tag{6d}$$

$$\dot{\alpha} = -\omega_1 + \omega_4 C\beta + \omega_6 S\beta, \tag{6e}$$

$$\dot{\beta} = -\omega_2 C\alpha - \omega_3 S\alpha + \omega_5, \tag{6f}$$

where

$$\lambda_i \equiv \omega_i - a_{i2}\dot{\psi}, \qquad i = 1,2,3, \tag{7}$$

and

$$\dot{\psi} = \Omega(1 - \epsilon^2)^{-\frac{3}{2}}(1 + \epsilon C\psi)^2. \tag{8}$$

If the ω_i's in (3a) through (3f) are treated as dependent variables, then (3a) through (3f) together with (6a) through (6f) form a system of 12 first-order equations in the 12 unknowns ξ, η, ζ, χ, α, β and ω_i, $i = 1, \cdots, 6$. This system of equations has been programmed on an IBM 7090 for numerical solutions for any given initial conditions and for given dimensionless parameters: satellite moment of inertia ratios I_i/I_2, $i = 1,3, \cdots, 6$, spring constants $k_i/I_2\Omega^2$, damping constants $\bar{C}_i = C_i/I_2\Omega$ (viscous damping) or $\bar{T}_{di}/I_2\Omega^2$, $i = 1,2$, $\bar{\alpha},\bar{\beta}$ (hysteresis damping). Some numerical results have been given in Ref. 1, while more numerical results are summarized in Section IV for parameter optimization in the case of hysteresis damping.

III. PARAMETER OPTIMIZATION WITH VISCOUS DAMPING

In the case of librational motion, the S_1-$x_1y_1z_1$ and S_2-$x_2y_2z_2$ axes oscillate about the earth-pointing rotating frame S_o-xyz with infinitesimal angles ξ_1, η_1, ζ_1 and ξ_2, η_2, ζ_2, respectively. Because of the universal joint constraint, we have $\alpha = \xi_2 - \xi_1$, $\beta = \eta_2 - \eta_1$, and $\zeta_2 = \zeta_1$. The position vector of the hinge in the S_1-$x_1y_1z_1$ coordinate system is $-L\hat{z}_1$, while in the S_2-$x_2y_2z_2$ it is zero. Let us assume that the orbital eccentricity, ϵ, is small compared with unity: i.e., ϵ is assumed to be of the same order as the infinitesimal angles, ξ_1, η_1, ζ_1, α, and β. Hence, from (8) one obtains $\dot\psi = \Omega + 2\epsilon\Omega C\Omega t + 0(\epsilon^2)$, $\psi = \Omega t + 2\epsilon S\Omega t + 0(\epsilon^2)$, and $\ddot\psi = -2\epsilon\Omega^2 S\Omega t + 0(\epsilon^2)$. Equations (3a) through (3f) can then be linearized in the case of viscous damping to two sets of equations in pitch and roll-yaw librations. Upon transformation of the independent variable from t to $\psi = \Omega t$, these equations become:

$$\frac{d^2\eta_1}{d\psi^2} - \frac{1}{I_2} T_{d2} + 3p_1\eta_1 - \bar{k}_2\beta = 2\epsilon S\psi, \quad (9a)$$

$$\frac{d^2\beta}{d\psi^2} + \frac{d^2\eta_1}{d\psi^2} + \frac{1}{I_5} T_{d2} + (3p_2 + \lambda\bar{k}_2)\beta + 3p_2\eta_1 = 2\epsilon S\psi. \quad (9b)$$

$$\frac{d^2\xi_1}{d\psi^2} - \frac{1}{I_1} T_{d1} + (1 - q_1)\frac{d\zeta_1}{d\psi} + 4q_1\xi_1 - \bar{k}_1\alpha = 0, \quad (10a)$$

$$\frac{d^2\alpha}{d\psi^2} + \frac{d^2\xi_1}{d\psi^2} + \frac{1}{I_4} T_{d1} + (1 - q_2)\frac{d\zeta_1}{d\psi}$$
$$+ (4q_2 + \mu\bar{k}_1)\alpha + 4q_2\xi_1 = 0, \quad (10b)$$

$$\frac{d^2\zeta_1}{d\psi^2} + (1 - f_1 - f_2)\zeta_1 - (f_1 + f_2)\frac{d\xi_1}{d\psi} - f_2\frac{d\alpha}{d\psi} = 0, \quad (10c)$$

where

$$T_{d1} = C_1\Omega^{-1}\frac{d\alpha}{d\psi}, \qquad\qquad T_{d2} = C_2\Omega^{-1}\frac{d\beta}{d\psi},$$

$$\bar{k}_1 = k_1/I_1\Omega^2, \qquad\qquad \bar{k}_2 = k_2/I_2\Omega^2,$$

$$\lambda = I_2/I_5, \qquad\qquad \mu = I_1/I_4,$$

$$p_1 = (I_1 - I_3)/I_2, \qquad\qquad p_2 = (I_4 - I_6)/I_5,$$

$$q_1 = (I_2 - I_3)/I_1, \qquad\qquad q_2 = (I_5 - I_6)/I_4,$$

$$f_1 = (I_1 + I_3 - I_2)/(I_3 + I_6), \quad\text{and}\quad f_2 = (I_4 + I_6 - I_5)/$$
$$(I_3 + I_6).$$

Note that (10c) is obtained by adding up the linearized versions of (3c) and (3f).

3.1 *Free Librational Motions*

For the free pitch libration, i.e., with $\epsilon = 0$ in (9a) and (9b), the stability criteria have been obtained in Ref. 1. To ensure that the earth-pointing frame, S_o-xyz, be the equilibrium position, it has been found that the spring constant should be larger than the following critical value:

$$\bar{k}_2{}^* = -\frac{3p_1 p_2}{\lambda p_1 + p_2} . \tag{11a}$$

Thus, the pitch spring constant $\bar{k}_2$ is chosen as

$$\bar{k}_2 = a\bar{k}_2{}^* = -\frac{3a p_1 p_2}{\lambda p_1 + p_2} , \tag{11b}$$

where $a > 1$. Similarly, the roll critical spring constant is found to be

$$\bar{k}_1{}^* = -\frac{4q_1 q_2}{\mu q_1 + q_2} , \tag{12a}$$

and the roll spring constant is chosen to be

$$\bar{k}_1 = b\bar{k}_1{}^* = -\frac{4b q_1 q_2}{\mu q_1 + q_2} , \tag{12b}$$

where $b > 1$. The characteristic equations in the complex variable s for the free pitch and roll-yaw librations are, respectively, of fourth order and sixth order:

$$s^4 + \bar{C}_2(1 + \lambda)s^3 + [3(p_1 + p_2) - 3a(\lambda + 1)p_1 p_2/(\lambda p_1 + p_2)]s^2$$
$$+ 3\bar{C}_2(\lambda p_1 + p_2)s + 9p_1 p_2(1 - a) = 0, \tag{13}$$

and

$$s^6 + \bar{C}_1(1 + \mu)s^5 + \left[\frac{(\mu - \lambda) + \lambda(1 - q_2)^2 + \mu\lambda(1 - q_1)^2}{\mu(\lambda + 1) - \lambda(\mu q_1 + q_2)} \right.$$
$$\left. + \frac{4q_2[q_2 - \mu(b - 1)q_1] + 4q_1[\mu q_1 - (b - 1)q_2]}{\mu q_1 + q_2} \right] s^4$$
$$+ \bar{C}_1 \left[\frac{(1 + \mu)(\mu - \lambda) + \lambda(1 - q_2)^2 + \mu\lambda(1 - q_1)(1 - q_2)}{\mu(\lambda + 1) - \lambda(\mu q_1 + q_2)} \right.$$

$$\left. + 4(\mu q_1 + q_2) + (1 - q_1)\mu\lambda \frac{\mu(1 - q_1) + (1 - q_2)}{\mu(\lambda + 1) - \lambda(\mu q_1 + q_2)}\right] s^3$$

$$+ 4\left[\frac{(\mu - \lambda)q_2[q_2 - \mu(b - 1)q_1]}{(\mu q_1 + q_2)\{\mu(\lambda + 1) - \lambda(\mu q_1 + q_2)\}}\right.$$

$$- \frac{b\mu\lambda q_1 q_2(1 - q_1)(1 - q_2)}{(\mu q_1 + q_2)\{\mu(\lambda + 1) - \lambda(\mu q_1 + q_2)\}} - 4(b - 1)q_1 q_2$$

$$\left. - (1 - q_1)\mu\lambda \frac{\left[\begin{array}{c}bq_1 q_2(1 - q_2)\\ - q_2(1 - q_1)[q_2 - \mu(b - 1)q_1]\end{array}\right]}{(\mu q_1 + q_2)\{\mu(\lambda + 1) - \lambda(\mu q_1 + q_2)\}}\right] s^2$$

$$+ 4\bar{C}_1 \frac{(\mu - \lambda)(\mu q_1 + q_2)}{\mu(\lambda + 1) - \lambda(\mu q_1 + q_2)} s + \frac{16 q_1 q_2(\mu - \lambda)(1 - b)}{\mu(\lambda + 1) - \lambda(\mu q_1 + q_2)} = 0.$$

(14)

In deriving (14) the satellite body has been assumed to be axisymmetric. The optimization problem for the free librational motions is such that by varying the parameters in the coefficients of (13) and (14) one gets the largest possible negative real part of the complex roots for the most slowly damped mode of librations. These parameters are $\bar{C}_2$, a, λ, p_1, and p_2 for the pitch motion, and $\bar{C}_1$, b, μ, q_1, and q_2 for the roll-yaw motion. The parameter λ contained in the roll-yaw characteristic equation is determined from the pitch optimization and is not treated as a varying parameter in the roll-yaw optimization. From the optimized values of the six parameters λ, μ, p_1, p_2, q_1, and q_2, one can determine the optimized inertia ratios I_i/I_2, $i = 1,3, \cdots, 6$. The value of I_2 is chosen from the magnitude of the gravitational torque at a given orbital altitude such that, in the presence of various environmental disturbing torques, the forced libration amplitude will not be larger than a specified value.

For a two-body satellite with geometric configuration of a dumbbell-sheet combination, we have

$$p_1 = 1, \qquad p_2 = -1, \qquad q_1 = 1, \qquad \text{and} \qquad q_2 = -1;$$

the characteristic equations are simplified to

$$s^4 + (1 + \lambda)\bar{C}_2 s^3 + 3a\frac{\lambda + 1}{\lambda - 1} s^2$$
$$+ 3(\lambda - 1)\bar{C}_2 s + 9(a - 1) = 0,$$

(15)

with parameters $\bar{C}_2$, a, and λ, and

$$s^6 + (1 + \mu)\bar{C}_1 s^5 + \left[\frac{4\lambda + (\mu - \lambda)}{\mu + \lambda} + \frac{4b(1 + \mu)}{\mu - 1} \right] s^4$$

$$+ \left[\frac{(1 + \mu)(\mu - \lambda) + 4\lambda}{\mu + \lambda} + 4(\mu - 1) \right] \bar{C}_1 s^3$$

$$+ 4 \left[\frac{b(\mu - \lambda)(1 + \mu) + 4\mu\lambda + 4\lambda(b - 1)}{(\mu - 1)(\mu + \lambda)} + 4(b - 1) \right] s^2 \qquad (16)$$

$$+ 4\bar{C}_1 \frac{(\mu - \lambda)(\mu - 1)}{\mu + \lambda} s + \frac{16(\mu - \lambda)(b - 1)}{\mu + \lambda} = 0,$$

with parameters $\bar{C}_1$, b, and μ. These two equations have been pro-
grammed on a digital computer for computation of complex roots with
$a,b = 1.0$ to 2.0, $\bar{C}_1$, $\bar{C}_2 = 0$ to 7.0, $\lambda = 1.25$ to 6.00, and $\mu = 2.0$ to
24.0. The case with $a,b < 1.0$ will give rise to positive real parts of the
roots and is of no interest to us.

The root loci of (15) and (16) are plotted in Figs. 4 and 5, respec-
tively, with fixed spring constants ($a = 1.2$, $b = 1.2$) and varying
damping constants and inertia ratios. The roots are plotted only in the
second quadrant of the complex plane, as they are complex conjugates
with negative real parts. In the case of critical and overcritical damping,
roots degenerate into the negative real axis. In the pitch case, with
$\lambda = 2/[3 - 5^{\frac{1}{2}}] \approx 2.61804$, the two distinct modes will, at $\bar{C}_2 \approx 1.2805$,
coalesce into a single point, $-n = -\mathrm{Re}(s) = -1.16$, on the negative
real axis, corresponding to a $1/e$ damping time of 0.137 orbit at large
t or ψ. This is the result given by Zajac.[3] For other values of λ, there
always exists a pair of complex conjugates for the two modes if $\bar{C}_2$ is
not too large. It is noted from Fig. 4 that when λ is in the range of 2.5 to
4.0, a proper choice of the damping constant $\bar{C}_2$ will make $-n_1$ of the
least damped mode not less than 0.7, which corresponds to a $1/e$ damp-
ing time of 0.23 orbit. Values of λ in the above range and the corre-
sponding optimum damping constants are given in Table I. This gives
the satellite designer a wide choice of the inertia ratio, I_2/I_5, and the
damping constant, $C_2/I_2\Omega$, and still the $1/e$ damping time is not greater
than 0.23 orbit in the free pitch libration case.

From the complex root-locus plot for the roll-yaw free libration (Fig.
5 at $b = \bar{k}_1/\bar{k}_1^* = 1.2$), it is noted that the highest and the intermediate
modes coalesce into a single point at $\mu \approx 6.425$, and $\bar{C}_1 \approx 0.3625$.
The corresponding lowest mode has a poor damping. The intermediate
and the lowest modes coalesce into a single point at $\mu \approx 18$ and $\bar{C}_1 \approx$
0.0935, which gives a poor damping for the highest mode. A close exami-
nation of the plot indicates that for μ lying in the range of 8 to 10,
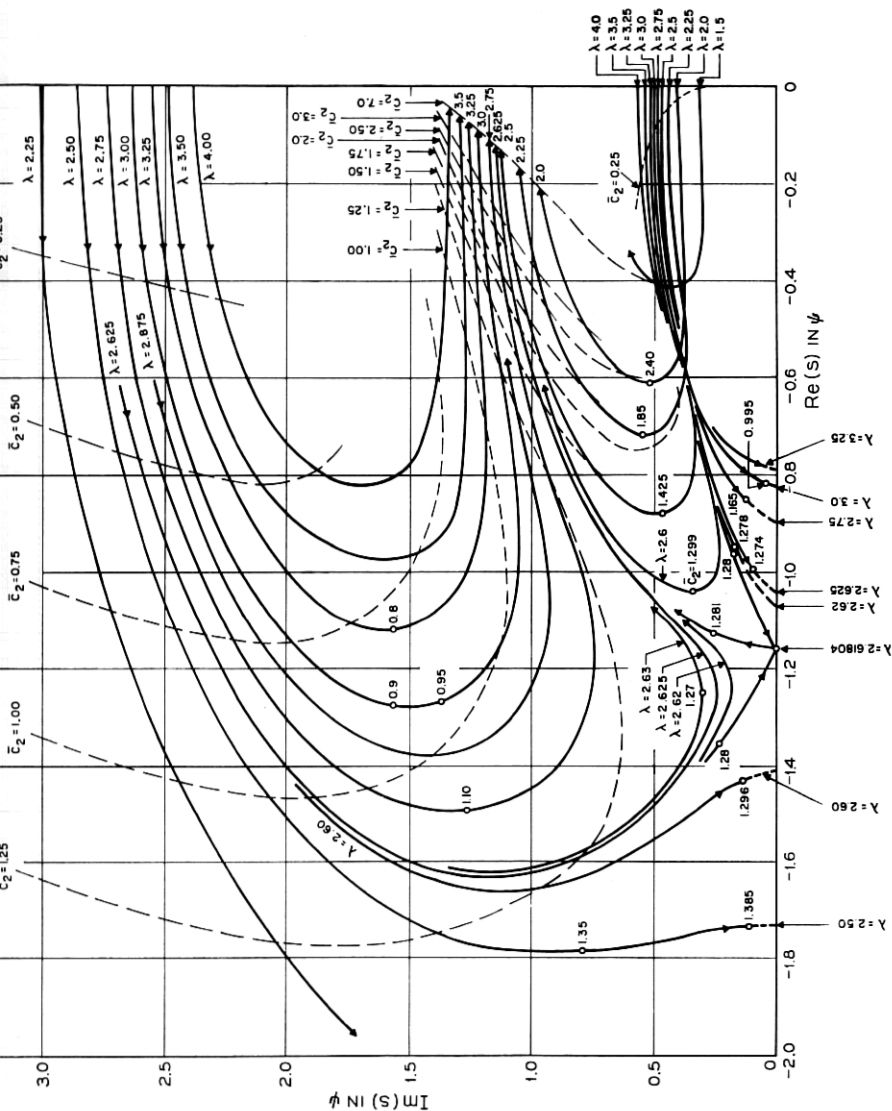
Fig. 4 — Complex root loci for pitch optimization with viscous damping ($a = \bar{k}_2/\bar{k}_2{}^* = 1.2$).
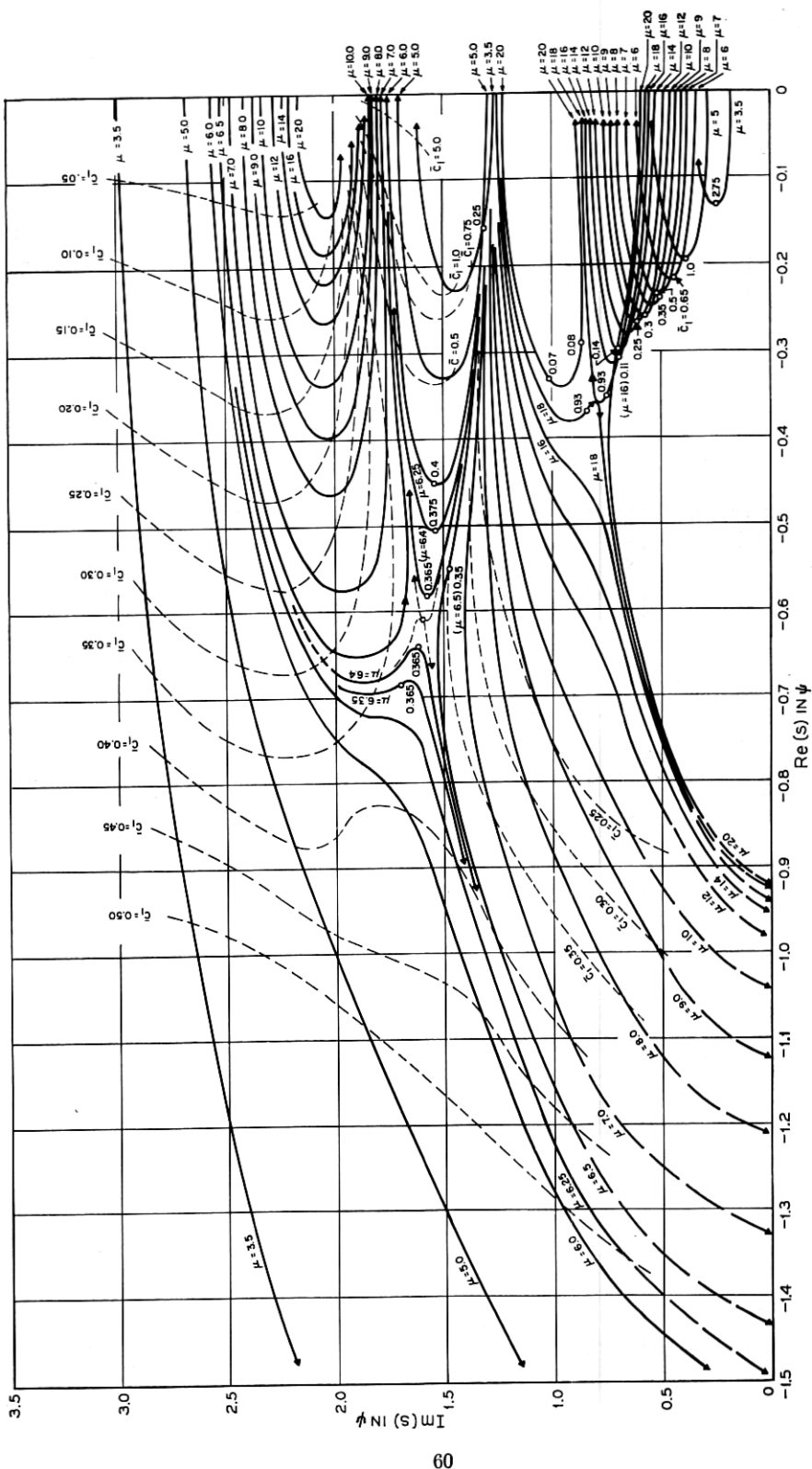
Fig. 5 — Complex root loci for roll-yaw optimization with viscous damping ($b = \bar{k}_1/\bar{k}_1^* = 1.2$).

60

TABLE I — OPTIMUM DAMPING CONSTANT OF PITCH LIBRATION

$\lambda \left(= \frac{I_2}{I_b} \right)$	$\bar{C}_2$	Negative Real Part in ψ, $-\mathrm{Re}(s)$	
		Lower Mode	Higher Mode
2.5	1.425	0.88	critically
2.6	1.299	1.04	damped
2.61804	1.2805*	1.16†	1.16
2.75	1.165	0.85	1.33
3.0	0.995	0.81	1.17
3.25	0.870	0.78	1.00
3.5	0.80	0.74	0.90
4.0	0.69	0.70†	0.75

* Both modes coalesce into a single point on the negative real axis.
† $\mathrm{Re}(s) = -1.16\psi$ corresponds to $1/e$ settling time of 0.137 orbit. $\mathrm{Re}(s) = -0.70\psi$ corresponds to $1/e$ settling time of 0.228 orbit.

a proper choice of the damping constant, $\bar{C}_1$, will make the negative real part of the least damped mode, $-\mathrm{Re}(s)_{\min}$, larger than 0.24, which corresponds to a $1/e$ damping time of 0.66 orbit. If the lower bound of $-\mathrm{Re}(s)_{\min}$ is relaxed to 0.20 ($1/e$ time $\approx$ 0.796 orbit), the range of μ becomes much wider, i.e., 6 to 14, as indicated in Table II with the corresponding optimum damping constant.

The variation of $-\mathrm{Re}(s)$ with the spring constants is such that the pitch optimum spring constant (for the least damped mode) depends on the choice of damping constant, $\bar{C}_2$, at a given inertia ratio, λ, as shown in Fig. 6 for a few chosen cases. In the roll-yaw case, the

TABLE II — OPTIMUM DAMPING CONSTANT OF ROLL-YAW LIBRATIONS

$\mu \left(= \frac{I_1}{I_4} \right)$	$\bar{C}_1$	Negative Real Part in ψ, $-\mathrm{Re}(s)$		
		Lowest Mode	Intermediate Mode	Highest Mode
6	0.65	0.216	0.211	critically damped
7	0.49	0.233	0.225	”
8	0.375	0.247	0.250	”
9	0.30	0.258	0.254	0.990
10	0.25	0.265	0.250	0.715
12	0.175	0.280	0.230	0.660
14	0.13	0.271	0.212	0.495

Note: $\mathrm{Re}(s) = -0.2\psi$ corresponds to $1/e$ settling time of 0.796 orbit. $\mathrm{Re}(s) = -0.28\psi$ corresponds to $1/e$ settling time of 0.568 orbit.
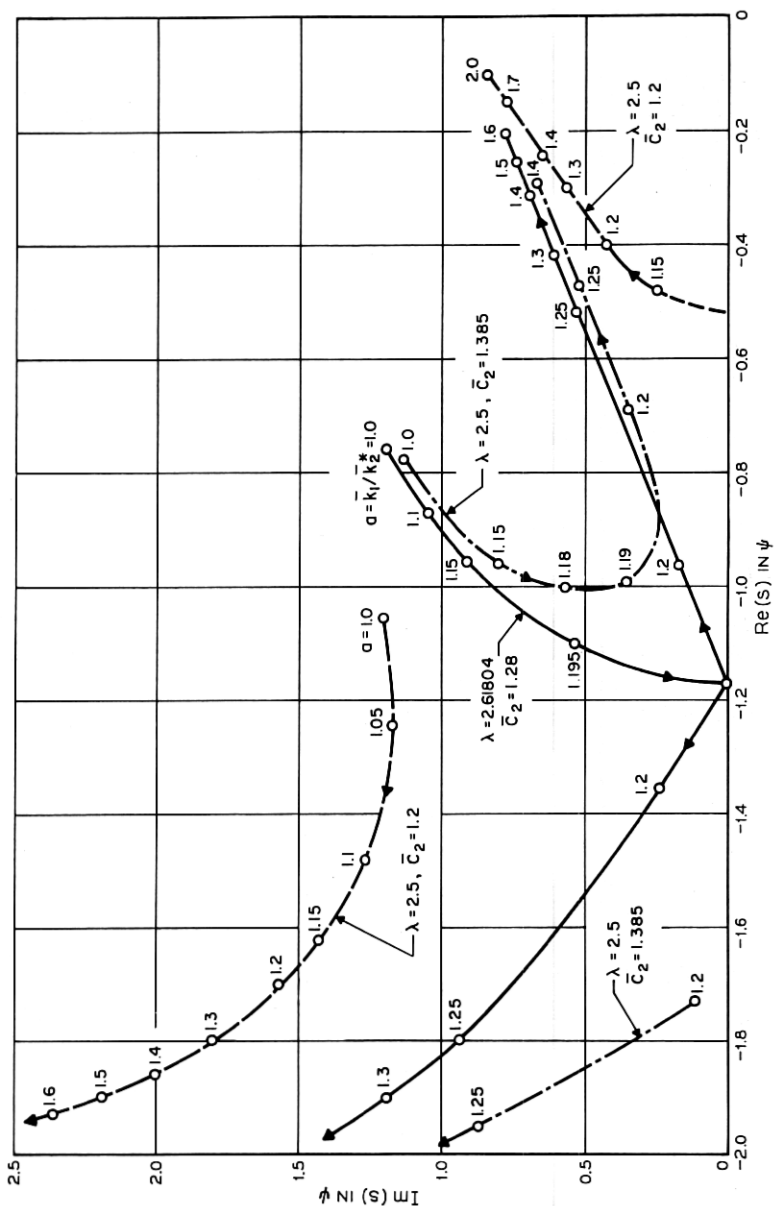
Fig. 6 — Variation of pitch damping with spring constants at fixed λ and $\bar{C}_2$.

optimum spring constant for the lowest mode is found always smaller than that for the intermediate mode, as indicated in Fig. 7, while the highest mode gets better damping for increased $\bar{k}_1$ or b. For example, at $\mu = 8.0$, and $\bar{C}_1 = 0.35$, optimum $\bar{k}_1$ equals 1.13 $\bar{k}_1^*$ for the lowest mode but equals 1.31 $\bar{k}_1^*$ for the intermediate mode. From a practical consideration of the spring design, one should not choose the spring constant too close to the critical value because of possible decrease due to vibrations, thermal effects, etc. Furthermore, an analysis of pointing errors resulting from deviations in geometric configuration (due to rod deflections,[1,2] etc.) indicates the advantage of employing larger spring constants. In view of these conflicting results, one may have to settle for some compromise values, e.g., $a,b \approx 1.2$ to 1.8.

3.2 *Forced Pitch Libration by Orbital Eccentricity*

The steady-state solution of (9a) and (9b) for η_1 is found to be

$$\eta_1 = F_1 C\psi + G_1 S\psi. \tag{17}$$

Here $F_1 = 2\epsilon\Delta^{-1}\bar{C}_2 P_2(P_1 - P_2)$, and

$$G_1 = 2\epsilon\Delta^{-1}[P_1 P_2^2 + (1 + 2\lambda)\bar{k}_2 P_1 P_2$$
$$+ \bar{k}_2 P_2^2 + (1 + \lambda)(\lambda P_1 + P_2)(\bar{C}_2^2 + \bar{k}_2^2)],$$

where $P_1 = 3p_1 - 1$, and $P_2 = 3p_2 - 1$. The ratio of the amplitude, $\bar{\eta}_1 = (F_1^2 + G_1^2)^{\frac{1}{2}}$, to the eccentricity, ϵ, is plotted in Fig. 8 versus the spring constant, a, with varying $\bar{C}_2$ and λ. This plot indicates the advantage of using a lower spring constant, and, for $1.0 < a \leq 1.4$, the advantage of employing a smaller damping constant. This latter advantage is further reflected in the plot of $\bar{\eta}_1/\epsilon$ versus $\bar{C}_2$ ($a = 1.2$) (Fig. 9), especially when λ is in the range of 2.5 to 3.5. It is noted from both Figs. 8 and 9 that at $\bar{C}_2 = 0.5$ ($a = 1.2$), $\bar{\eta}_1/\epsilon$ is relatively independent of λ. If the optimum damping constant for the free librational motion, as given in Table I, for $\lambda = 2.5$ to 4.0 is used, the average value of $\bar{\eta}_1/\epsilon$ is approximately 2.25, which is only about 30 per cent larger than that given by $\bar{C}_2 = 0.5$.

IV. PARAMETER OPTIMIZATION WITH MAGNETIC HYSTERESIS DAMPING

4.1 *Energy-Fitting Method*

In the case of magnetic hysteresis damping, the equations of librational motions are the same as (9a) and (9b) for pitch, and (10a)
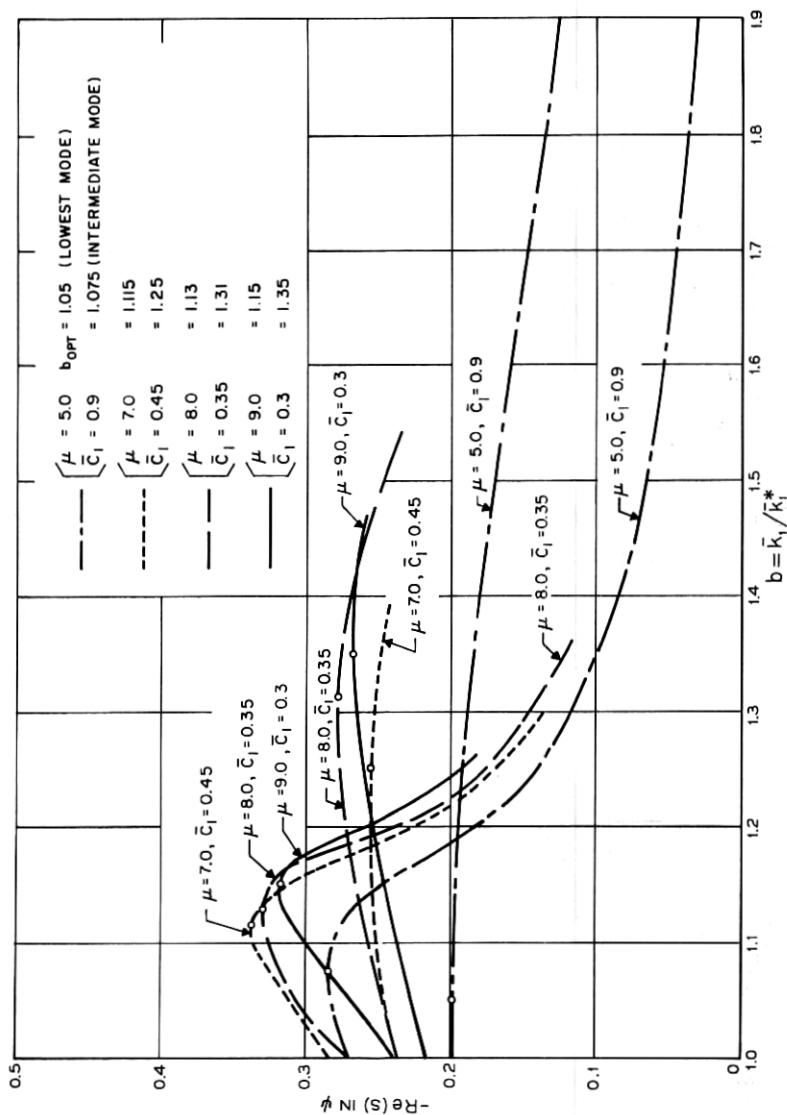
Fig. 7 — Variation of roll-yaw damping with spring constants at fixed μ and $\bar{C}_1$.
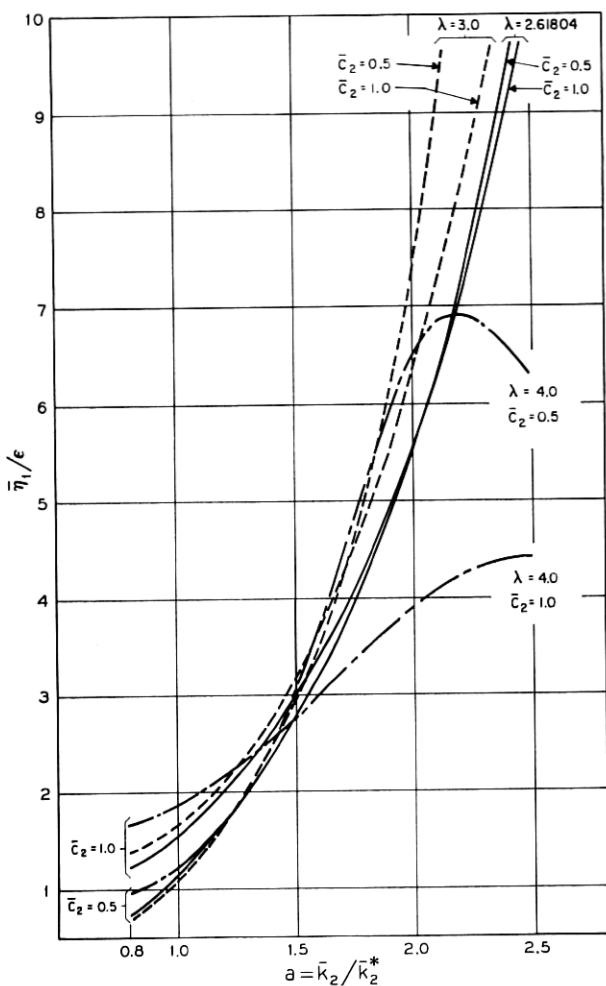
Fig. 8 — $\bar{\eta}_{1/}\epsilon$ vs a with varying λ and $\bar{C}_2$.

through (10c) for roll and yaw, except that the damping torques T_{d1} and T_{d2} become nonlinear and may be defined as follows. If, for example, the pitch relative angle of rotation from a neutral position, β, is larger then $\bar{\beta}$, then the major hysteresis loop (see Fig. 3) will be traced, and (5) will be applied for the pitch damping torque. If however, β is less than $\bar{\beta}$ after a change of sign of $\dot{\beta}$, then the torque will in general trace a minor loop as, for example, that shown in Fig. 10. The maximum
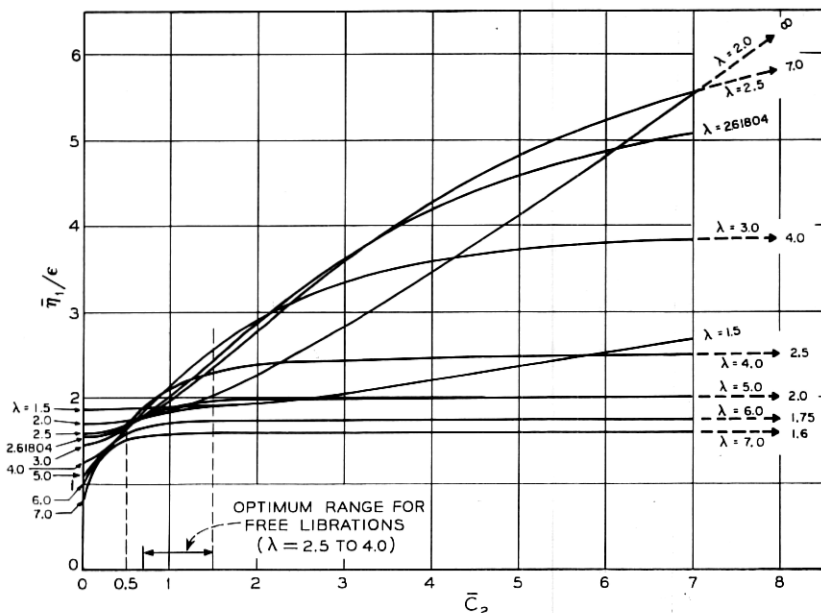
Fig. 9 — $\bar{\eta}_1/\epsilon$ vs $\bar{C}_2$ with varying λ ($a = \bar{k}_2/\bar{k}_2{}^* = 1.2$).

magnitude of the torque in the minor loop may be a function of the angular excursion. Since the torque always opposes the motion, the plot of the torque versus time is a broken curve (see Fig. 10). Each section of the curve can be represented by an analytical expression if it is approximated as a section of a rhomboid or an ellipse. Such an approximation can be used for numerical integration of the equations of motion.

If the T_{d2}-β curve is approximated as a closed loop for a slowly damped system, the loop area which represents the energy of dissipation per cycle of oscillation, E_h, is related to the angular amplitude of oscillation β as follows:

$$E_h = 4\bar{T}_{d2}(\beta - \bar{\beta}) \qquad \text{for} \qquad \beta \geqq \beta_0, \tag{18a}$$

and

$$E_h = K\bar{T}_{d2}\beta^m \qquad \text{for} \qquad \beta < \beta_0. \tag{18b}$$

In the above, $\bar{\beta}$, β_0, K, and m are constants depending on the characteristics of the damping material, etc., where $\bar{\beta}$ and β_0 are found usually to be very small, e.g., $\bar{\beta} = 1°$ to $4°$, and $\beta_0 = 3°$ to $7°$. If one equates E_h to the energy dissipation per cycle with the viscous damping,

$E_v = \pi C_2 \omega \beta^2$ ($\omega =$ circular frequency of one of the principal modes) at a certain value of β, then a relation between $\bar{C}_2$ and $\bar{T}_{d2}$ results. For example, when $E_h = E_v$ at $\beta = \beta_0$, then

$$\frac{\bar{T}_{d2}}{I_2 \Omega^2} = \left[\frac{\pi}{4} \frac{\beta_0^2}{(\beta_0 - \bar{\beta})} \frac{\omega}{\Omega} \right] \bar{C}_2. \tag{19}$$

A similar relation can be obtained between $\bar{C}_1$ and $\bar{T}_{d1}/I_1\Omega^2$. Thus, from the "optimum" viscous damping constants obtained in Section III, one may find the equivalent "optimum" hysteresis damping torque. Nevertheless, it is pointed out that the equivalent "optimum" $\bar{T}_d$ obtained in such a way could be erroneous for the following reasons. First, this is not a slowly damped system, as can be observed from the computer solutions[1] of equations (3) with hysteresis damping, and also, as can be noted from Figs. 4 and 5, $\mathrm{Re}(s)$ is of the same order as $\mathrm{Im}(s)$ in the case of viscous damping. Hence, a closed-loop approximation for computing E_h and E_v based on a particular frequency is obviously a very poor one. Second, since the quadratic curve for E_v can fit the E_h-curve ($m \approx 1.5$ power for $\beta \leqq \beta_0$ and linear for $\beta \geqq \beta_0$) at only one point (see Fig. 11), (19) gives a much worse approximation at other values of β than at the point of fit.

4.2 Numerical Method — Computer Solutions

From the foregoing, it is apparent that "optimum" magnetic hysteresis damping constant cannot be accurately evaluated from the "opti-
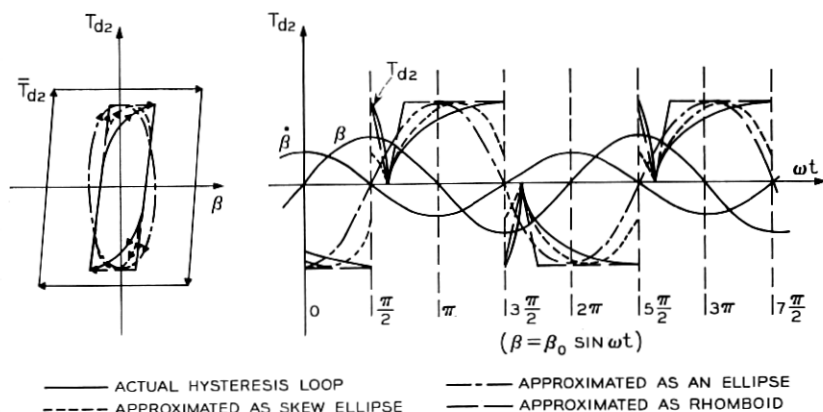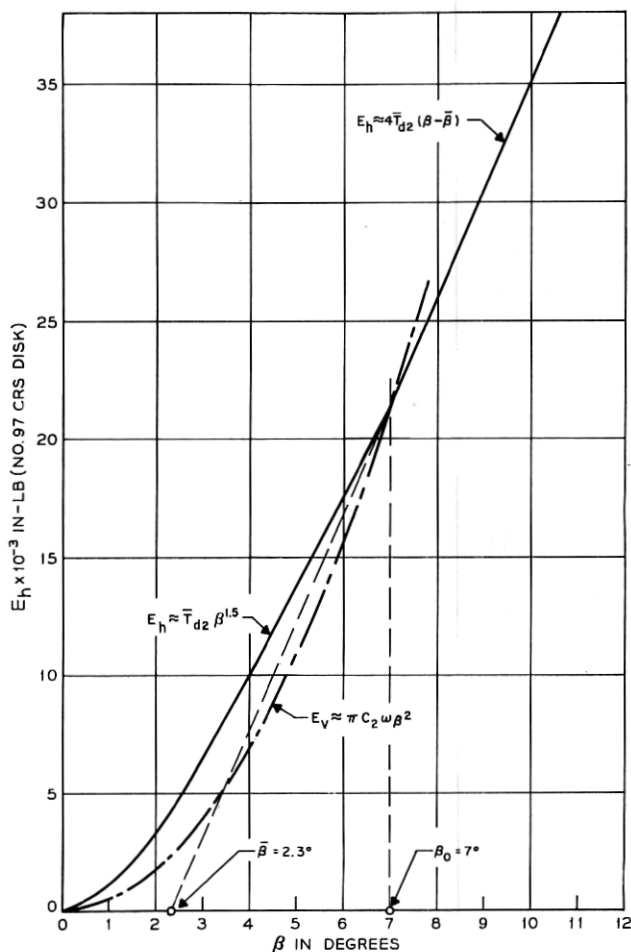

Fig. 10 — Minor magnetic hysteresis loops: torque-time diagram.

Fig. 11 — E_h-β curve.

mum" viscous damping constant by means of the energy method or other approximation methods, such as, the describing function method[*] (for example, see Ref. 4). Therefore, in the case of hysteresis damping, it is necessary to resort to numerical methods for the parameter optimi-

---

[*] If one defines the equivalent gain as the ratio of the first harmonics of the output, hysteresis damping torque, to the amplitude of the oscillation angle, assumed to be sinusoidal, and equates it to $C_1 s$ or $C_2 s$ in the characteristic equations, then the equations will only have terms of even power with, however, complex coefficients. This method is actually the same as the energy-fitting method and clearly offers no advantages.

zation. The results obtained in Section III for the viscous damping case may, however, be used as a guide. It is found from the computer solutions that the critical spring constants (11a) and (12a) obtained from the linearized equations (9a), (9b), and (10a) through (10c) with the viscous damping apply also for the case of hysteresis damping. It has also been demonstrated by computer solutions that the values of the inertia ratios, λ and μ, in the ranges given in Tables I and II, will give better damping for the same hysteresis damping torques and spring constants. We shall numerically integrate (3a) through (3f) and (6a) through (6f) with the hysteresis damping torque defined in (5) by putting $\bar{\alpha}$ and $\bar{\beta}$ equal to 1° to 4°. This eliminates the unnecessary complex programming of the minor loops of the hysteresis damping, though no damping will result when α and β are smaller than $\bar{\alpha}$ and $\bar{\beta}$, respectively. If the initial condition is a tumbling motion, the numerical results will cover tumbling motion, large-angle motion, and librational motion. Only in the librational motion does the solution get less and less accurate when the relative angles get closer to $\bar{\alpha}$ and $\bar{\beta}$.
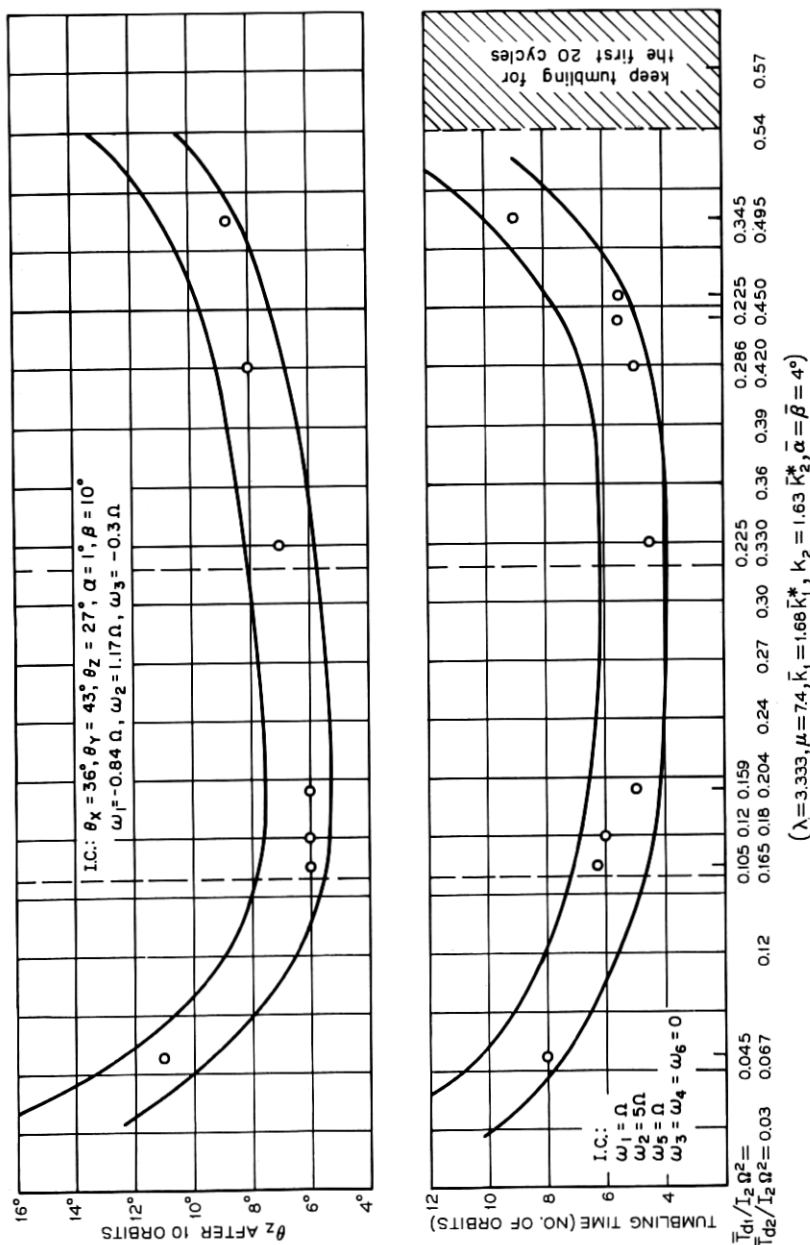
A number of computer runs have been made employing hysteresis damping constants in a wide range. The results indicate: (a) the number of orbits after which the satellite will stop tumbling from the initial condition, $\omega_1 = \Omega$, $\omega_2 = 5\Omega$, $\omega_5 = \Omega$, $\omega_3 = \omega_4 = \omega_6 = 0$; and (b) the librational angles after 20 orbits. Computer runs have also been made (for the case of $\lambda = 3.333$, $\mu = 7.4$ only) to determine the librational angles after 10 orbits from the initial condition: at $t = 0$, $\theta_x = 36°$, $\theta_y = 43°$, $\theta_z = 27°$, $\alpha = 1°$, $\beta = 10°$, $\omega_1 = -0.84\Omega$, $\omega_2 = 1.17\Omega$, $\omega_3 = -0.3\Omega$. These angles are defined as $\theta_x = C^{-1}(\hat{x}_1 \cdot \hat{x})$, $\theta_y = C^{-1}(\hat{y}_1 \cdot \hat{y})$, and $\theta_z = C^{-1}(\hat{z}_1 \cdot \hat{z})$, (the caret denotes a unit vector), where θ_z is the earth-pointing error angle. The results of these computer runs are summarized in Figs. 12 through 14 for three sets of inertia ratios.

It is noted from Figs. 12–14 that the damping constants which give better damping in librations are, in general, smaller than those for better tumbling damping. Poor damping will result in both tumbling and librational motions when $\bar{T}_{d1}$ and $\bar{T}_{d2}$ are either too small or too large. In the intermediate wide range of the damping constants there is relatively small variation in the damping time. The "optimum" damping constants may be chosen from this wide range as, for example,

$$\bar{T}_{d2}/I_2\Omega^2 = \begin{cases} 0.19 - 0.38 & \text{for} \quad \lambda = 2.62, \quad \mu = 6.28 \\ 0.16 - 0.32^* & \text{for} \quad \lambda = 3.33, \quad \mu = 7.4 \\ 0.08 - 0.16 & \text{for} \quad \lambda = 4.0, \quad \mu = 14, \end{cases}$$

---

* The upper limit is taken to be smaller than that given in Ref. 2.
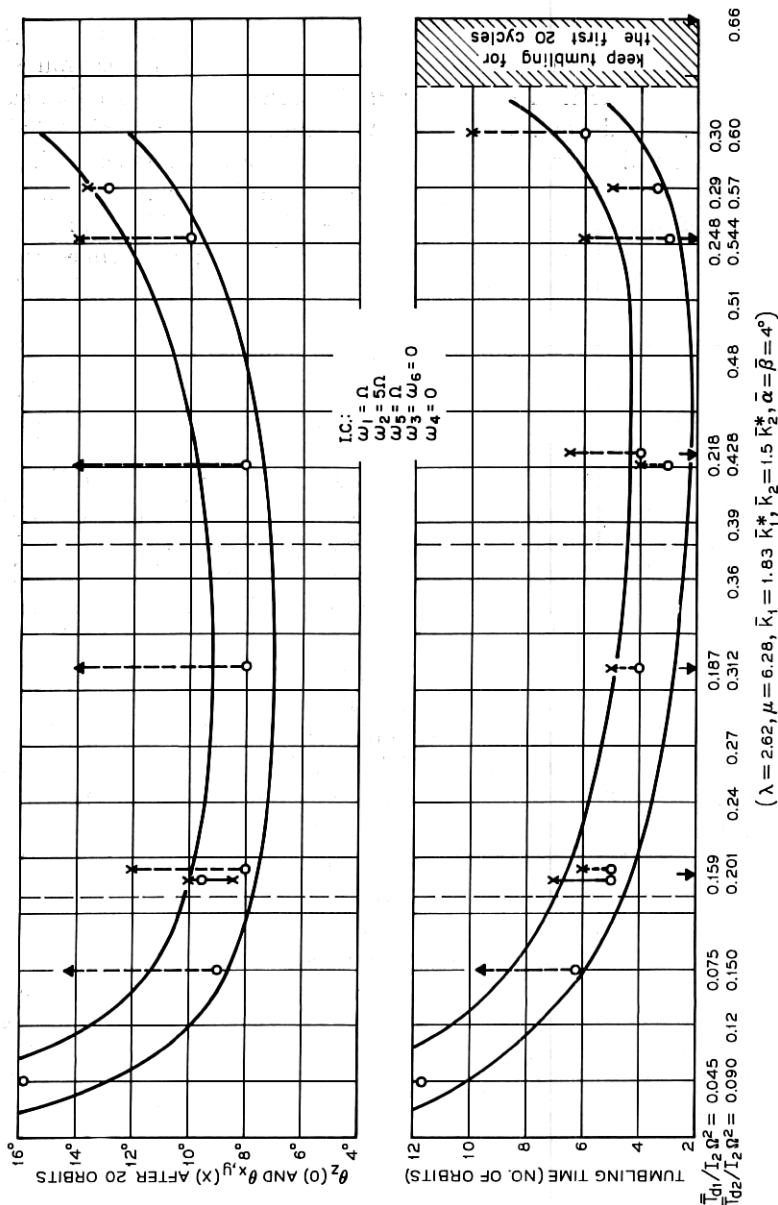
Fig. 12 — Computer results with magnetic hysteresis damping, $\lambda = 2.62$, $\mu = 6.28$.

Fig. 13 — Computer results with magnetic hysteresis damping, $\lambda = 3.333$, $\mu = 7.4$.
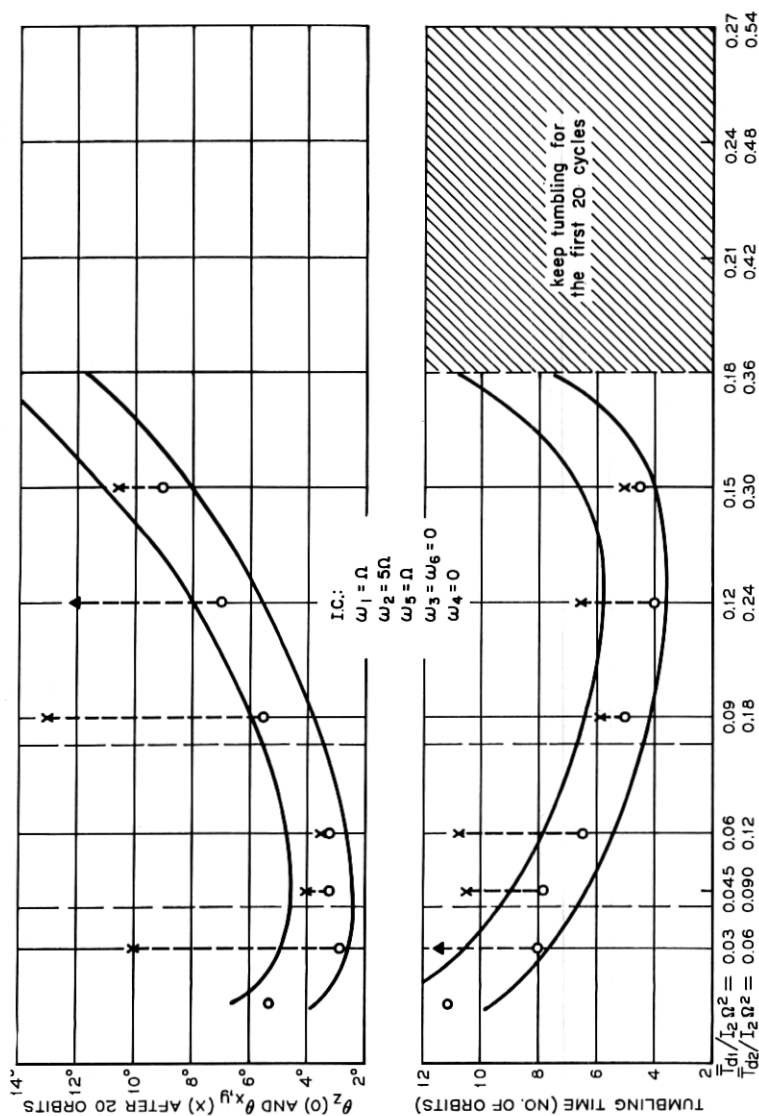
Fig. 14 — Computer results with magnetic hysteresis damping, $\lambda = 4$, $\mu = 14$.

and $\bar{T}_{d1}$ is chosen to be one-half of $\bar{T}_{d2}$. Since only a limited number of computer runs have been made, it is not possible to display $\bar{T}_{di}/I_2\Omega^2$ ($i = 1,2$) as a function of $\lambda(= 2.5 \text{ to } 4.0)$ and $\mu(= 6 \text{ to } 14)$. The "optimum" damping constants corresponding to other values of λ and μ have yet to be determined from computer runs.

The effects of spring constants have also been investigated on the computer by varying the spring constants under the same hysteresis damping constants. It is found that the variation in damping time is relatively small for $\bar{k}_i/\bar{k}_i{}^* = 1.2 \text{ to } 1.8$ ($i = 1,2$). The lower limit is chosen to guarantee stability.[1] To ensure torsional fatigue strength of the torsion wire, it is preferable to choose high spring constants. Furthermore, employment of larger spring constants will reduce the error angle in case of rod bending, as indicated in the error analysis.

The relation between the forced librational amplitude and the orbital eccentricity has been found from the computer runs to be

$$\theta_z \approx 2\epsilon \text{ to } 3\epsilon$$

for $\epsilon \leq 0.10$. At $\epsilon = 0.2$, the satellite starts tumbling from an earth-pointing position after 1.5 orbits, whereas at $\epsilon = 0.4$ tumbling begins immediately after the start.

Due to the nonlinear characteristics, the effectiveness of the magnetic hysteresis damping cannot be measured by the $1/e$ settling time as with viscous damping. However, an equivalent $1/e$ settling time for the hysteresis damping may be obtained in the following way. Take, for example, a typical computer run as plotted in Fig. 15 for $\theta_z[\lambda = 4, \mu = 14, \bar{T}_{d1}/I_2\Omega^2 = 0.06, \bar{T}_{d2}/I_2\Omega^2 = 0.12, \bar{k}_i = 1.4\bar{k}_i{}^* (i = 1,2), \bar{\alpha} = \bar{\beta} = 2°]$. From the envelope curve of the amplitudes of the damped large-angle motion, the logarithmic decrements can be approximately evaluated by taking the motion as exponentially damped. It is found that the equivalent $1/e$ time ranges from one to three orbits with an average of two orbits. Within the validity of the librational motion, this represents an average $1/e$ time for both pitch and roll-yaw librations with the above parameters.

V. SUMMARY — ILLUSTRATION OF A PRACTICAL DESIGN

The results given in the previous sections indicate that there does not exist a single set of optimum parameters which give the best over-all damping performance. However, there have been found relatively wide optimum ranges of the inertia ratios, the spring constants, and the damping constants for the design of a two-body satellite. The optimum
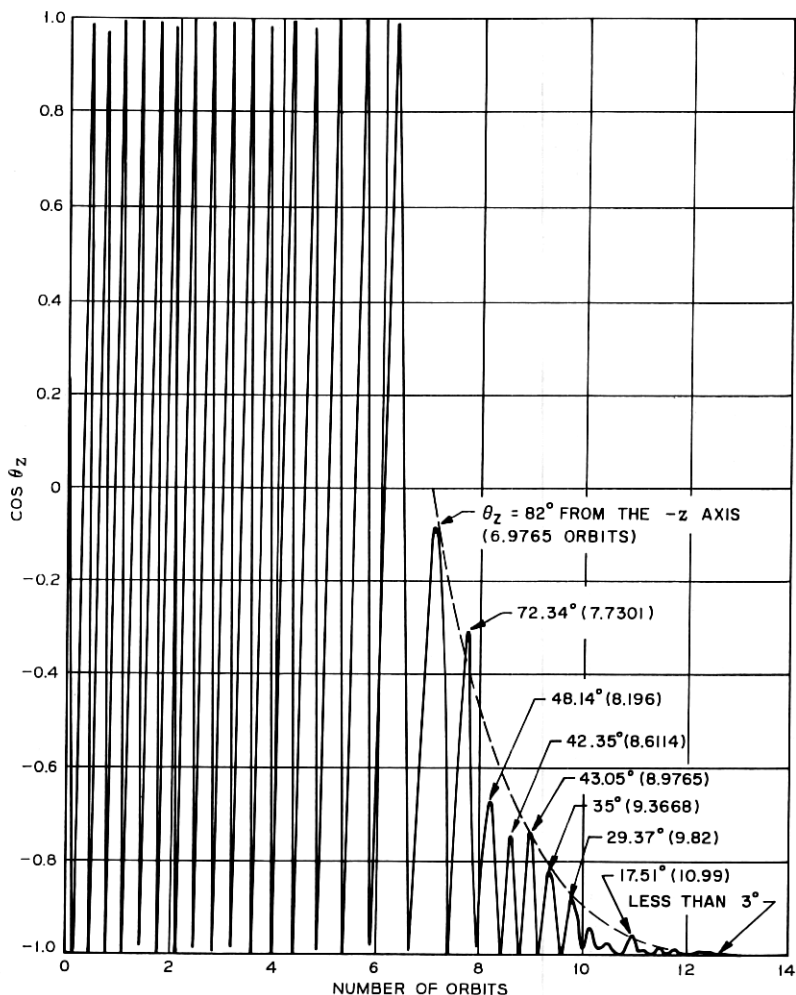
Fig. 15 — Variation of θ_z with magnetic hysteresis damping.

ranges of the inertia ratios and the spring constants are found applicable to both viscous and magnetic hysteresis damping. They are λ ($= I_2/I_5$) = 2.5 to 4.0, μ ($= I_1/I_4$) = 6 to 14, and $\bar{k}_{1,2}/\bar{k}_{1,2}{}^* = 1.2$ to 1.8. The optimum viscous damping constants, as tabulated in Tables I and II, can be read directly from the complex root-locus plots, whereas the optimum ranges of the magnetic hysteresis damping constants corresponding to a few inertia ratios are obtained from the computer runs.

As far as the inertia ratios are concerned, it is advantageous to employ large λ and μ so that the deck rods[2] can be made shorter or the tip mass can be smaller. By employing shorter deck rods and furthermore by shortening the mast rod,[2] it is possible to balance out the solar torque, which was the largest disturbing torque for the satellite described in Ref. 2. As long as the solar torque is reduced to a small magnitude, the lowered gravity torque level resulting from the shortening of the mast rod will not substantially increase the error angles produced by other relatively small disturbing torques. In view of the foregoing, we could improve the design previously given in Ref. 2. The parameters may now be chosen as follows:

$I_1 = I_2 = 600, I_3 = 10$ slug-ft^2

pitch gravity torque, $T_g = 0.23 \times 10^{-5}$ ft-lb/deg $= 31$ dyne-cm/deg

$\lambda = 4, I_5 = 150; \mu = 14, I_4 = 42.8$ slug-ft^2

$\bar{T}_{d1}/I_2\Omega^2 = 0.06, \bar{T}_{d1} = 0.446 \times 10^{-4}$ ft-lb

$\bar{T}_{d2}/I_2\Omega^2 = 0.12, \bar{T}_{d2} = 0.892 \times 10^{-4}$ ft-lb

$\bar{k}_1 = 1.8 \bar{k}_1^* = 0.55, k_1 = 0.247 \times 10^{-4}$ ft-lb/rad

$\bar{k}_2 = 1.8 \bar{k}_2^* = 1.8, k_2 = 0.804 \times 10^{-4}$ ft-lb/rad

length of mast rod $= 30$ ft (assuming 160-lb satellite proper)

length of deck rod $= 16.5$ ft (4 deck rods)

roll tip mass $= 2 \times 2.5 = 5$ lbs

pitch tip mass $= 2 \times 9 = 18$ lbs

total mass for attitude control (excluding mast motor and support) $= 26$ lbs.

The solar torque error angle is now only 1°, and the total error angle is found to be about 4° excluding the effect of the orbit eccentricity:

magnetic dipole moment (TELSTAR's)	2°
solar torque	1°
rod bending (silver-plated rod)	1°
orbital eccentricity, ϵ	2ϵ to 3ϵ
total	$4° + 2.5\epsilon$.

In the preceding, the error angle due to the residual magnetic dipole moment can be easily reduced to 1° or less by further refinement of the cancellation techniques used on the TELSTAR satellite.

REFERENCES

1. Fletcher, H. J., Rongved, L., and Yu, E. Y., Dynamics Analysis of a Two-Body Gravitationally Oriented Satellite, B.S.T.J., **42**, Sept., 1963, pp. 2239–2266.

2. Paul, B., West, J. W., and Yu, E. Y., A Passive Gravitational Attitude Control System for Satellites, B.S.T.J., **42,** Sept., 1963, pp. 2195–2238.
3. Zajac, E. E., Damping of a Gravitationally Oriented Two-Body Satellite, ARS Jour., **32,** pp. 1871–1875, Dec., 1962.
4. Gibson, J. E., *Nonlinear Automatic Control*, McGraw-Hill, New York, 1963, Chap. 9.